ULTRASTRUCTURAL CHARACTERISTICS OF SPERMIOGENESIS IN *RHYNCHOPHORUS FERRUGINEUS* (COLEOPTERA: CURCULIONIDAE)

ABDULLAH M. ALZAHRANI[1,*], SALAHELDIN A. ABDELSALAM[1,2], OMAR M. ELMENSHAWY[1,3] AND ASHRAF M. ABDEL-MONEIM[1,4]

[1]Department of Biological Sciences, Faculty of Science, King Faisal University, Hofouf, Saudi Arabia

[2]Zoology and Entomology Department, Faculty of Science, Assiut University, Egypt

[3]Department of Zoology, Faculty of Science, Al-Azhar University, Egypt

[4]Department of Zoology, Faculty of Science, University of Alexandria, Egypt

*Corresponding author; E-mail: aalzahra@kfu.edu.sa

ABSTRACT

The red palm weevil (RPW), *Rhynchophorus ferrugineus* Olivier (Coleoptera: Curculionidae), is a pest that is rapidly spreading across the globe. Here, the ultrastructure of *R. ferrugineus* spermatogenesis and sperm are described. The histology of the testis, sperm ultrastructure, and spermiogenesis were investigated using light and transmission electron microscopy. The differentiation of spermatids was observed to occur within spermiogenetic cysts. Inside each cyst, the spermatids were at the same stage of maturation. During early stages, mitochondria aggregated, fused, and elongated beside the growing flagellar axoneme, while the proacrosome transformed into a triple-layered acrosome, with a perforatorium, acrosomal vesicle, and extra-acrosomal layer. The centriolar adjunct was present in early spermatids but was absent from later spermatid stages and sperm. The sperm's tail displayed a typical axoneme with a 9 + 9 + 2 microtubule arrangement, 2 mitochondrial derivatives of unequal size, and 2 accessory bodies. A small number of sperms exhibited twin or multiple tails due to membrane fusion. Our results support systematic relationships within the family Curculionidae.

Key Words: axoneme, acrosome, spermatogenesis, microtubules, nebenkern, pterygote spermatozoa, ultrastructure, red palm weevil

RESUMEN

El picudo rojo (RPW), *Rhynchophorus ferrugineus* Olivier (Coleoptera: Curculionidae), es una plaga que se está extendiendo rápidamente en todo el mundo. Se describe la ultraestructura de la espermatogénesis y los espermatozoides de *R. ferrugineus*. Se investigó la histología de los testículos, ultraestructura de espermatozoides y espermatogénesis, con microscopía óptica y de transmisión electrónica. Se observó que la diferenciación de las espermátidas ocurre dentro de los quistes spermiogenéticos. Dentro de cada quiste, las espermátidas se encontraban en la misma fase de maduración. Durante las primeras etapas, los mitocondrias se agregaron, juntaron, y alargaron al lado del axonema flagelar creciente, mientras que el proacrosoma se transformó en un acrosoma de tres capas, con un perforatorium, vesícula acrosomal y la capa extra-acrosomal. El complemento centriolar estuvo presente en las primeras espermátidas, pero estuvo ausente en las etapas posteriores de los espermátidas y espermatozoides. La cola del espermatozoide pareció como un axonema típico con un 9 + 9 + 2 disposición de microtúbulos, 2 derivados mitocondriales de tamaño desigual y 2 cuerpos auxiliares. Un pequeño número de espermatozoides exhibió colas dobles o múltiples debido a la fusión de la membrana. Nuestros resultados apoyan las relaciones sistemáticas dentro de la familia Curculionidae.

Palabras Clave: axonema, acrosoma, espermatogénesis, microtúbulos, nebenkern, espermatozoides pterygotes, ultraestructura, picudo rojo

The red palm weevil (RPW), *Rhynchophorus ferrugineus* Olivier (Coleoptera: Curculionidae), is one of the most destructive pests of coconuts and date palm trees in the world (Faleiro et al. 2003). Its larvae feed on the interior tissues of the palm trunk, destroying the tree. Currently, *R. ferrugineus* is widely distributed in Oceania, the Near, Middle, and Far East (Li et al. 2009), and Europe and America (Dembilio & Jacas 2012).

Rhynchophorus ferrugineus spermatogenesis was briefly described by Bartlett (1983). The spermatozoa of most Coleoptera, especially the Curculionidae, display the classic structure, which is characterized by a head region formed by a 3-layered acrosome and nucleus. Two enormous accessory bodies and 2 large and crystallized mitochondrial derivatives support the tail region. A 9 + 9 + 2 axoneme pattern is the most common pattern within the Curculionidae (Gassner et al. 1975; Burrini et al. 1988; Name et al. 2007; Werner & Simmons 2011). Only the Rynchiitidae exhibit an axoneme pattern of 9 + 9 + 0 (Burrini et al. 1988). The number of curculionid species is overwhelming. Therefore, it is difficult to construct systematic lines based on phylogenetic data. However, accumulation of spermatological information on Curculionid species can aid in understanding spermatogenesis in these destructive pests and help to resolve taxonomic and phylogenetic discrepancies among them.

The aim of the current study is to provide a detailed understanding of *R. ferrugineus* spermiogenesis through elucidation of the sperm ultrastructure using light and electron microscopy techniques and to compare it to published data on other related species.

Materials and Methods

Insect Culture

The insects used in this study were obtained from infested palm trees in the Alahsa area of eastern Saudi Arabia. The insects were cultured in a rearing room at 25 ± 2 °C , 70 ± 5% RH and 12:12 h L:D. Sugarcane was used to feed the larvae, while the adults were reared on sugarcane pieces and cotton wicks saturated with a 10% sugar solution for feeding and egg laying.

Light Microscopy

Testes were dissected in Ringer's physiological solution and fixed in a 10% formalin solution overnight. The specimens were washed, dehydrated, and cleared in xylene before being embedded in paraffin wax. Multiple serial sections, with a thickness of 5 μm, were obtained and stained with hematoxylin and eosin. The sections were observed with a Nikon 80i light microscope (Nikon, Tokyo, Japan).

Free spermatozoa were obtained by dissecting testes in phosphate buffer saline (pH 7.2) and fixed in 4% paraformaldehyde. Sperm smears were stained with Harris's Haematoxylin and mounted in a drop of DPX.

Transmission Electron Microscopy

For electron microscopic examination, small pieces of testicular tissues were fixed at 4 °C in a 3% glutaraldehyde solution buffered with 0.1 M sodium cacodylate at pH 7.2, then post-fixed in 1% osmium tetroxide in the same buffer for 2 h, dehydrated in a graded series of ethanol, transferred to propylene oxide, and embedded in an Epon-Araldite mixture. Ultra-thin sections were obtained using diamond knives with a Leica EM UC6 ultramicrotome (Leica Co., Vienna, Austria). The samples were subsequently stained with 2% uranyl acetate and lead citrate prior to examination on a Jeol JEM 1011 transmission electron microscope (Jeol Ltd., Tokyo, Japan) at 80 kV.

Image Analysis

Quantitative analysis of sperm dimensions were detected using the freeware ImageJ v1.33 downloaded from the NIH website (http://rsb.info.nih.gov/ij).

The figures in this articled are also shown in the supplementary material for this article in Florida Entomologist 96(4) (December 2013) online at http://purl.fcla.edu/fcla/entomologist/browse .

Results

Rhynchophorus ferrugineus males had 2 testes, which were subdivided into tubular testicular follicles, and each follicle was enclosed by a layer of epithelial cells (Fig. 1). The follicles were filled with cysts at various stages of development. The outer rim of the testis was occupied by zones containing spermatogonia, while zones containing spermatocytes and spermatids were situated internally. Numerous spermatozoa were observed in the lumen of deferent duct using light microscopy. The sperm cells of *R. ferrugineus* appeared linear and very thin with an overall length of 87.23 ± 14.12 μm (mean ± standard deviation, n = 9) (Fig. 2). The headpiece measured approximately 10.12 ± 1.19 μm in length (n = 14), comprising about 10% of the total sperm length.

Inside spermiogenetic cysts, all spermatids were in the same stage of maturation. During the early spermatid phase, the nucleus was similar to that of somatic cells, displaying dispersed chromatin with some electron-dense areas. The early spermatids contained many mitochondria, expanded Golgi complexes and some smooth
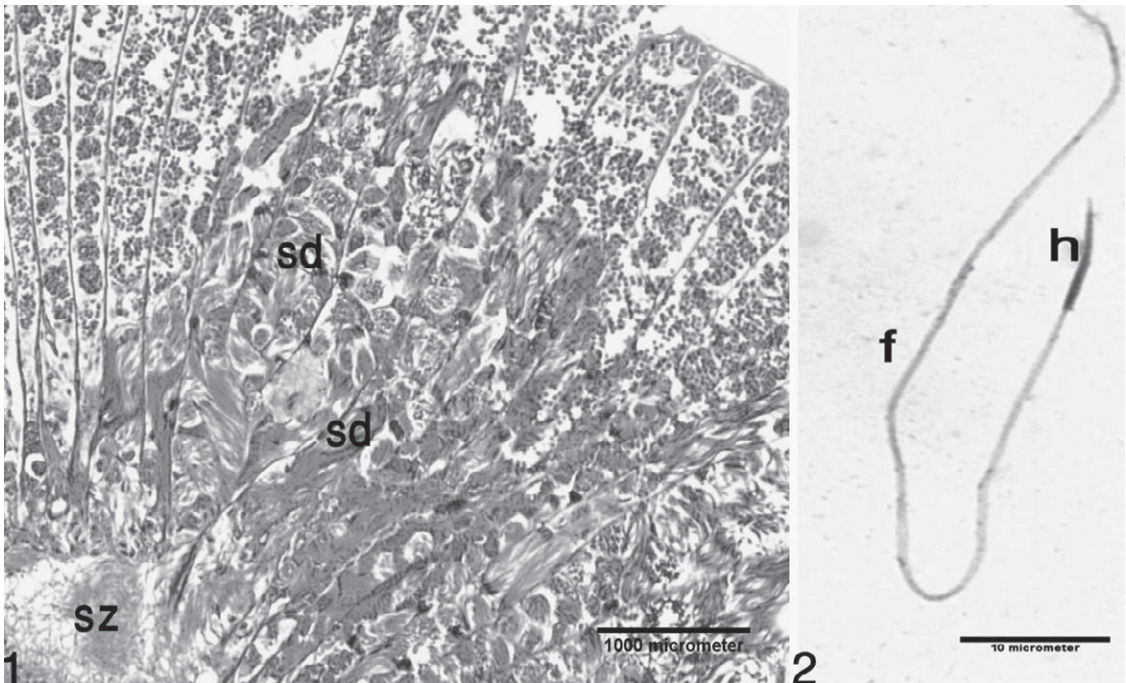
Figs. 1-2. Spermiogenesis in *Rhynchophorus ferrugineus*. (1) A longitudinal section of the testis of *R. ferrugineus* showing a large number of follicles per testis. Note the bundles of spermatids (sd) inside the mature cysts within the follicles; sz = spermatozoa in the lumen of deferent duct. Hematoxylin and eosin staining. (2) Whole spermatozoon of *R. ferrugineus* with distinct head (h) and flagellum (f). Harris haematoxylin staining. These two figures are shown in color in the supplementary material for this article in Florida Entomologist 96(4) (December 2013), which is online at http://purl.fcla.edu/fcla/entomologist/browse .

endoplasmic reticulum cisternae. The mitochondria were aggregated into 2 parts (Fig. 3), which were fused together, giving rise to 2 conspicuous nebenkerns in a juxtanuclear position (Fig. 4). An acrosome vesicle, derived from the Golgi complex, was observed near the nuclear envelope (Fig. 5). In this phase, an electron-dense material, the centriole adjunct, began to accumulate around the centriole in the region of flagellum implantation (Fig. 6). During the intermediary stages of spermatic maturation, there was a gradual condensation of nuclear chromatin, causing an increase in electron density. The structural reorganization of chromatin during nuclear condensation does not follow the same course in all insect species, and chromatin condensation was not uniform in *R. ferrugineus*. During some stages, the region near the nuclear envelope contained homogeneously condensed chromatin, while the central region was distinguished by the presence of chromatin fibers (Fig. 7). Thus, nuclear chromatin condensed gradually, and large blocks were associated with the nuclear envelope (Fig. 8). In mature spermatids, we observed a compact nucleus surrounded by a layer of manchette microtubules, and there were small spots of less electron-dense areas within the chromatin mass (Fig. 9). Simultaneous with chromatin condensation and nuclear and cellular elongation, the acrosomic complex covered the anterior of the nucleus, and development of the flagellum was initiated, with the centriolar adjunct disappearing in late spermatid stages (Fig. 10). The axoneme elongated from a centriole (Fig. 11), and 2 mitochondrial derivatives developed from the nebenkern toward the posterior end and exhibited cristae that were arranged perpendicular to the axoneme (Fig. 12). During the formation of the mitochondrial derivatives, these structures were separated from each other, and there were microtubules present in the surrounding cytoplasm (Fig. 13). These 2 structures showed different sizes, and the larger one exhibited a dense crystalloid in the mitochondrial matrix in the region opposite the axoneme (Fig. 14). The mitochondrial derivatives in the tail region were also associated with a well-developed agranular endoplasmic reticulum (ER). Laterally, on both sides of the axoneme, 2 electron-dense arches were observed. Some testicular cysts contained bi- or multi-flagellate spermatids with 2 or more axonemes. In the bi- or tri-flagellate varieties, 2 to 3 nebenkern derivatives were noted (Fig. 15).
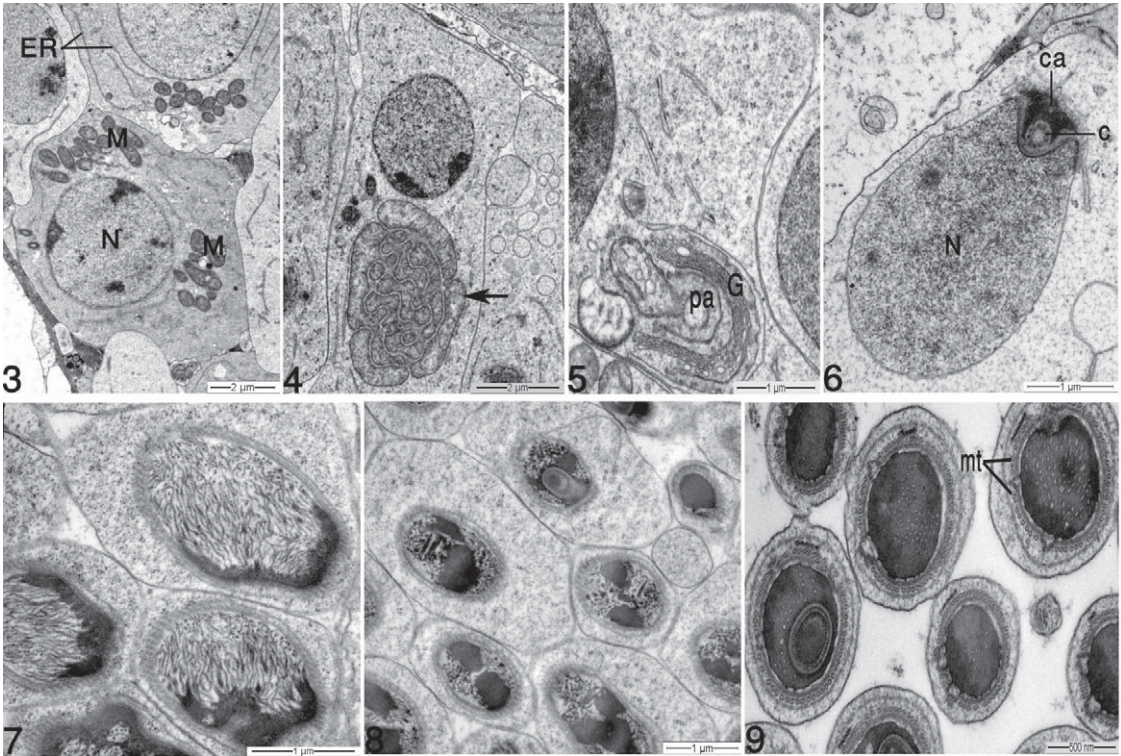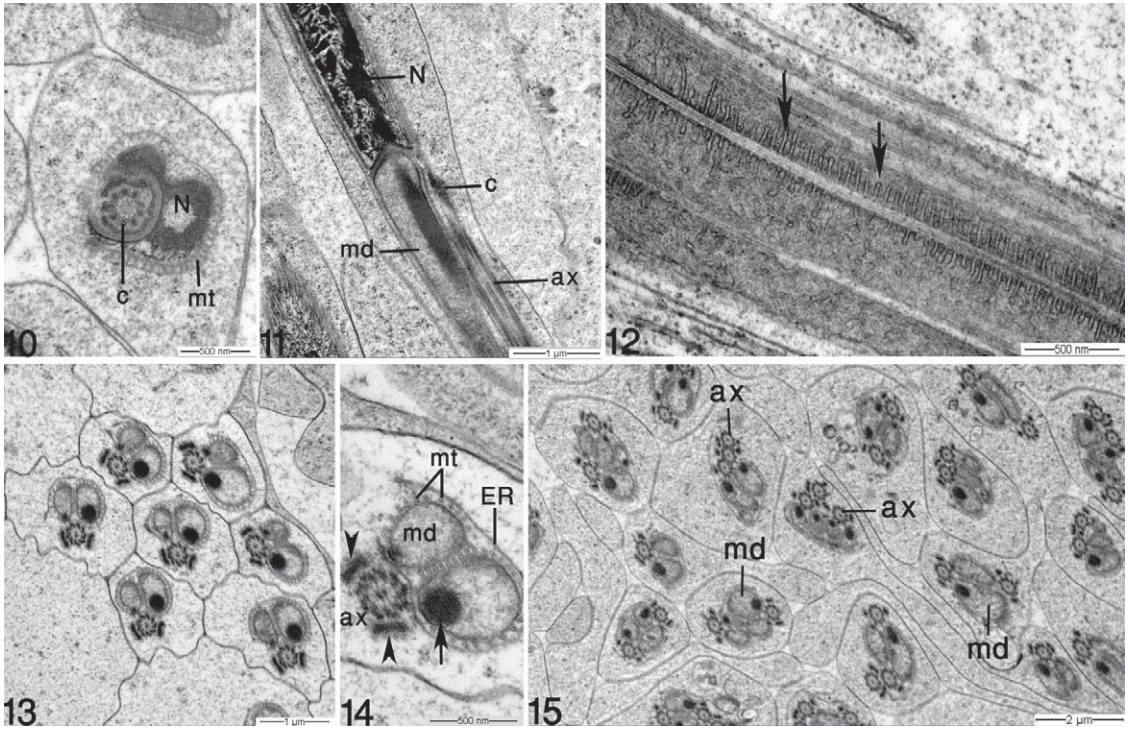
Figs. 3-9. Transmission electron micrographs of *Rhynchophorus ferrugineus* spermatids. (3) C.S. of early spermatids containing a nucleus (N), a cluster of mitochondrial masses (M), and cisternae of the smooth endoplasmic reticulum (ER). (4) The mitochondrial nebenkern (arrow) is evident in a later stage of spermiogenesis. (5) A proacrosomal vesicle (pa) and Golgi membranes (G) are observed near the nucleus. (6) The centriolar region in the initial stage of spermatid differentiation showing the nucleus (N), the centriolar adjunct material (ca), and the centriole (c). (7-9) The chromatin shows gradual condensation at the nuclear periphery, converging into the nuclear central region; mt = microtubules.

The spermatozoon of *R. ferrugineus* had a homogenously dense nucleus (Fig. 16). The diameter of the nucleus was reduced progressively from 0.81 to 0.32 μm before its apex was reached. When examined via electron microscopy, the cone-shaped acrosome was very short (about 1.24 μm in length) and triple layered; the perforatorium-like inner core was surrounded by electron-dense acrosomal contents, which was itself covered by an extra-acrosomal layer (Fig. 17). The transition between the basal part of the perforatorium and the anterior part of the nucleus was visible (approximately 25 nm). In cross-sections, the acrosome displayed profiles that varied from circular to oval (data not shown). The flagellar region included an axoneme, a pair of mitochondrial derivatives, a pair of triangular accessory bodies, and a puff-like corpuscle with electron-dense areas (Fig. 18). In addition, the mitochondria derivatives were about 0.33 μm at their widest diameter. In the axoneme, we observed a 9 (outer singlets) + 9 (intermediate doublets) + 2 (central singlets) pattern of microtubules. Twin or multiple sperm tails were also observed (Fig. 19). In these cases, each axoneme was part of a distinct flagellum.

DISCUSSION

Although spermiogenesis and spermatozoan morphology are similar among most insect species, many species also exhibit certain distinctive characteristics. In this report, the ultrastructural aspects of spermiogenesis in *R. ferrugineus* are described. The spermatozoa of *R. ferrugineus* largely follow the generalized model of pterygote spermatozoa proposed by Baccetti (1972). The arrangement of the mitochondrial cristae and the quantity and distribution pattern of electron-dense material within the mitochondrial derivatives are characteristic of each species (Baccetti 1972; Rosati et al. 1976). In *R. ferrugineus*, the nuclei of early spermatids were observed to be displaced to the cell periphery, while the nebenkern concentrated at the opposite pole to form 2 clusters. In contrast, only one nebenkern cluster is found in the tenebrionid beetle, *Palembus der-*

Figs. 10-15. Transmission electron micrographs of *R. ferrugineus* spermatids. (10) C.S. of the nuclear-flagellum transition in late spermatids. At this level, the centriolar adjunct is absent. N = nucleus, ax = tail axonemes, c = centriolar region, mt = microtubules. (11) L.S. of late spermatids. The centriole (c) lies posterior to the nucleus, and the axoneme (ax) emerges from it. The mitochondrial derivative (md) is later positioned at the axoneme. (12) L.S. of mitochondrial derivatives, showing a region of cristae (arrows). (13) C.S. through the flagellar region of mono-flagellate spermatids. (14) Higher magnification of the spermatid flagellum. The axoneme (ax) consists of a complex of 9+9+2 microtubules. Beneath the axoneme, 2 unequal mitochondrial derivatives (md) are evident, with advanced crystallization (arrow) being observed in the larger one. Lateral to the axoneme, 2 characteristic dense arches (arrowheads) are visible. Note also that microtubules (mt) mostly surround the axoneme and the mitochondrial derivatives. ER = agranular ER. (15) Group of bi- and tri-flagellate spermatids in an advanced state. Two to 3 mitochondrial derivatives (md) are visible.

mestoides Fairm (de Almeida et al. 2000). The presence of 2 mitochondrial derivatives of different sizes, as observed in *R. ferrugineus*, is common among many coleopteran species and many other insect orders (Báo et al. 1993b; Name et al. 2007).

The gradual condensation of the nuclear material is accompanied by a change in the shape of the nucleus from spherical to elongated. During the elongation of the nucleus, the chromatin is reorganized, resulting in a long, highly compact nucleus. In some instances, the nucleus contains small spots of less electron-dense areas within the chromatin mass, rather than a homogeneous texture. The nuclear material does not undergo uniform morphological changes during spermiogenesis, as either the central zone or the periphery can be the first to condense (Chevailler 1970). Similar structural changes during nuclear development have been described in other beetles

(Báo et al. 1993a; Báo 1996; Name et al. 2007). The microtubular manchette around the elongating nucleus observed in the *R. ferrugineus* (Fig. 9) is also present in the beetle *Tenebrio molitor* L. (Wolf et al. 1995). The acrosome of *R. ferrugineus* displays 3 layers, similar to that of the Curculionidae *Sitophilus zeamais* (Motschulsky), and *Sitophilus oryzea* (L.) (Name et al. 2007) and the featherwing beetle, *Bambara* sp. (Coleoptera: Ptiliidae) (Dybas et al. 1987). The presence of a centriolar adjunct in the spermatid stage and its absence in the mature sperm are also similar to what is observed in *S. zeamais* and *S. oryzea* (Name et al. 2007) as well as *T. molitor* (Baccetti et al. 1973) and *Anthonomus grandis* Boheman (Gassner et al. 1975). The axoneme pattern of 9 + 9 + 2 found in *R. ferrugineus* is another common coleopteran feature (Name et al. 2007). Weevils of the family Rhynchitidae (Curculionoidea) provide the only exception to this rule, as they display a
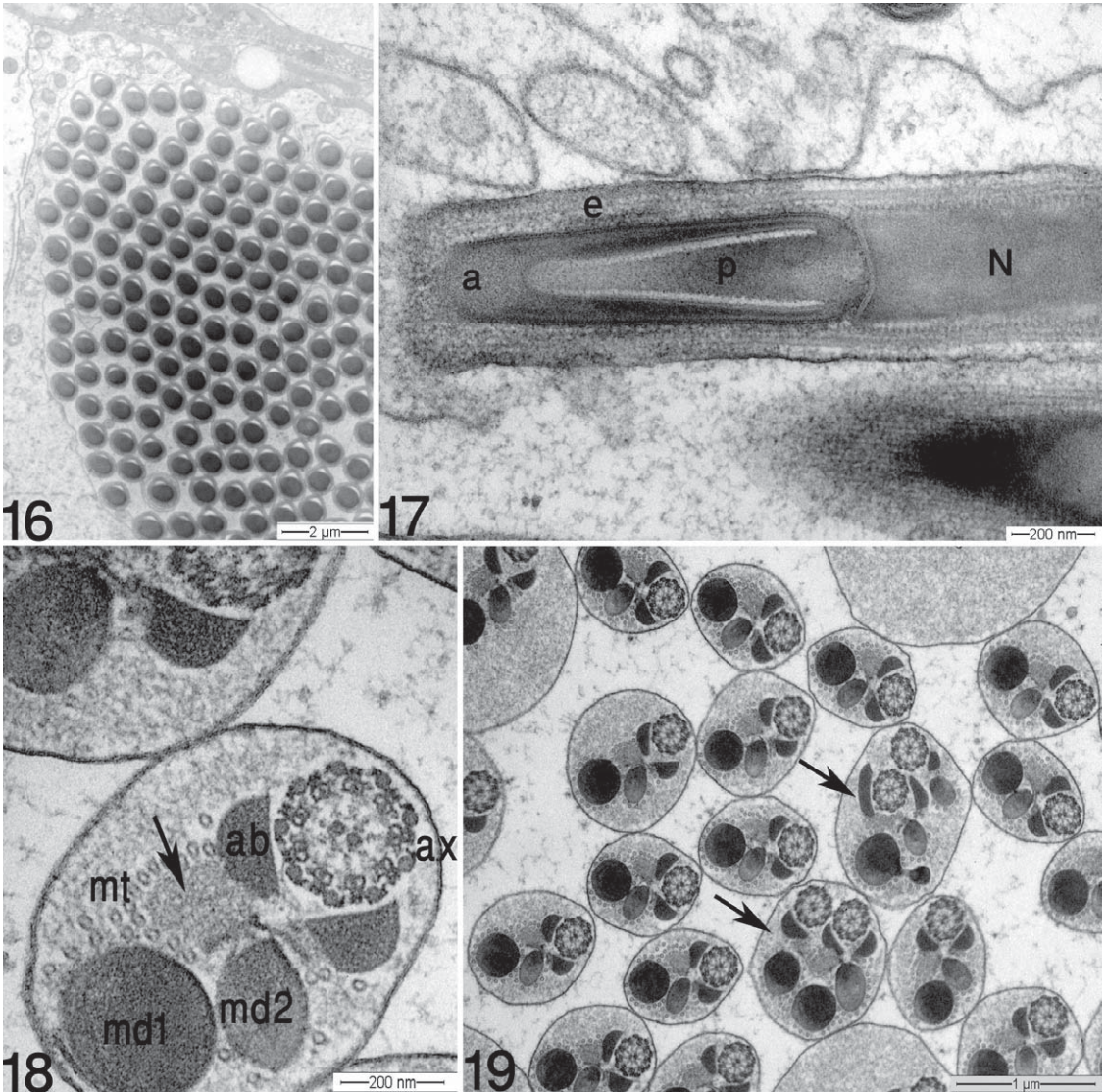
Figs. 16-19. Transmission micrographs of *R. ferrugineus* spermatozoa. (16) Cyst containing a C.S. of the spermatozoa head region. (17) L.S. of a sperm head showing the perforatorium (p), acrosomal vesicle (a), and extra-acrosomal tissue (e). N = nucleus. (18) C.S. of a sperm flagellum showing the 9+9+2 axoneme (ax), accessory bodies (ab), mitochondrial derivatives (large md1 and small md2), and the puff-like corpuscle (arrow). Mt = microtubules. (19) Arrows indicate bi-flagellate sperm with 2 axonemes.

9 + 9 + 0 axoneme pattern and a limited degree of asymmetry in the tail organelles (Burrini et al. 1988). The flagellum of *R. ferrugineus* exhibits 2 equal-sized accessory bodies and one puff-like corpuscle, which are common characteristics in most coleopterans, except in the flagellum of *Coelomera lanio* Dalman and *Cerotoma arcuata* (Olivier) (Coleoptera: Chrysomelidae), which present a single accessory body (Báo 1996, 1998). The puff-like corpuscles, with a flocculent aspect, exhibit different shapes and sizes. Similar structures have been observed in other Chrysomelidae

(Baccetti & Daccordi 1988) and Curculionoidea (Burrini et al. 1988; Name et al. 2007). The puff-like corpuscles seem to be characteristic components of the coleopteran flagellum, and it is likely that these corpuscles help to maintain the equilibrium of the flagellar structure during motility (Name et al. 2007).

In the present study, bi- and multi-flagellate spermatids and spermatozoa were observed at a low rate. This phenomenon is common in insects (Wolf 1997), although it is not observed in the Curculionidae *S. zeamais* and *S. oryzea* (Name et

al. 2007). One explanation for this phenomenon, introduced by Wolf (1997), is that there may be a secondary fusion of cells, which could occur during gonial mitosis, where a complex system of cytoplasmic bridges connects the germ cells throughout spermatogenesis. The cytoplasmic bridges widen occasionally, and cells fuse with one another. Another possibility is that supernumerary chromosomes (B chromosomes) may be present, which would increase the incidence of cell fusion during spermatogenesis (Suja et al. 1987, 1989). To our knowledge, only 5 weevil species have been reported to exhibit B chromosomes (Ennis 1972; Smith & Brower 1974; Dey 1989; Holecová et al. 2005). Determining the specific reason for the existence of bi- and multi-flagellate sperm in *R. ferrugineus* will require further investigation.

References Cited

Baccetti, B. 1972. Insect sperm cells. Adv. Insect Physiol. 9: 315-397.

Baccetti, B., Burrini, A. G., Dallai, R., Giusti, F., Mazzini, M., Renieri, T., Rosati, F., and Selmi, G. 1973. Structure and function in the spermatozoon of *Tenebrio molitor*. The spermatozoon of Arthropoda XX. J. Mechanochem. Cell Motil. 2: 149-161.

Baccetti, B., and Daccordi, M. 1988. Sperm structure and phylogeny of the Chrysomelidae, pp. 357-378 *In* P. Jolivet, E. Petitpierre and T. H. Hsiao [eds.], Biology of Chysomelidae. Academic Press, Kluwer.

Bartlett, A. C., and Rananavare, H. D. 1983. Karyotype and sperm of the red palm weevil (Coleoptera: Curculionidae). Ann. Entomol. Soc. Am. 76: 1011-1013.

Báo, S. N., and Hamú, C. 1993a. Nuclear changes during spermiogenesis in two chrysomelid beetles. Tissue Cell 25: 439-445.

Báo, S. N., and De Souza W. 1993b. Ultrastructural and cytochemical studies of the spermatid and spermatozoon of *Culex quinquefasciatus* (Culicidae). J Submicrosc. Cytol. Pathol. 25: 213-222.

Báo, S. N. 1996. Spermiogenesis in *Coelomera lanio* (Chrysomelidae: Galerucinae) ultrastructural and cytochemical studies, pp. 119-132 *In* P. Jolivet and M. L. Cox [eds.], Chrysomelidae Biology: General Studies. Academic Publishers, Netherlands.

Báo, S. N. 1998. Ultrastructural and cytochemical studies on spermiogenesis of the beetle *Cerotoma arcuata* (Coleoptera, Chrysomelidae). Biocell 22: 35-44.

Burrini, A. G., Magnano, L., Magnano, A. R., Scala, C., and Baccetti, B. 1988. Spermatozoa and phylogeny of Curculionoidea (Coleoptera). Intl. J. Insect Morphol. Embryol. 17: 1-50.

Chevailler, P. 1970. Le noyau du spermatozoïde et son evolution au cours de la spermiogenèse, pp. 499-514, *In* B. Baccetti [ed.], Comparative Spermatology. Accademia Nazionale dei Lincei. Academic Press, New York and London.

De Almeida, M. C., and Da Cruz-Landim, C. 2000. Spermeiogenesis in *Palembus dermestoides* (Coleoptera: Tenebrionidae) with emphasis on the formation of mitochondrial derivatives. Brazilian. J. Morphol. Sci. 17: 75-80.

Dembilio, O., and Jacas, J. A. 2012. Bio-ecology and integrated management of the red palm weevil, *Rhynchophorus ferrugineus* (Coleoptera: Curculionidae), in the region of Valencia (Spain). Hellenic Plant Protect. J. 5: 1-12.

Dey, S. K. 1989: B-chromosomes in two species of Indian weevils (Coleoptera: Curculionidae). Cytobios 57: 15-18.

Dybas, L. K., and Dybas, H. 1987. Ultrastructure of mature spermatozoa of a minute featherwing beetle from Sri lanka (Coleoptera, Ptiliidae: *Bambara*). J. Morphol. 191: 63-76.

Ennis, T. J. 1972. Low chromosome number and post reductional X0 in *Gelus californicus* (Lec.) (Coleoptera: Curculionidae). Canadian J. Genet. Cytol. 14: 851-857.

Faleiro, J. R., Rangnekar, P. A., and Satarkar, V. R. 2003. Age and fecundity of female red palm weevils *Rhynchophorus ferrugineus* (Olivier) (Coleoptera: Rhynchophoridae) captured by pheromone traps in coconut plantations of India. Crop Prot. 22: 999-1002.

Gassner, G., Childrem, D., and Klemetson, D. J. 1975. Spermiogenesis in boll weevil *Anthonomus grandis* Boheman (Coleoptera: Curculionidae). Intl. J. Insect Morphol. Embryol. 4: 15-25.

Holecová, M., Rozek, M., and Lachowska D. 2005. Evidence of B-chromosomes in the karyotype of *Barypeithes pellucidus* Boheman 1834 (Coleoptera, Curculionidae, Entiminae) from Central Europe. Folia Biol. (Krakow). 53: 65-68.

Li, Y., Zhu, Z., Ju R., and Sheng Wang, L. 2009. The red palm weevil, *Rhynchophorus ferrugineus* (Coleoptera: Curculionidae), newly reported from Zhejiang, China and update of geographical distribution. Florida Entomol. 92: 386-387.

Name, K., Dos Reis, G., and Báo S. 2007. An ultrastructural study of spermiogenesis in two species of *Sitophilus* (Coleoptera: Curculionidae). Biocell 31: 229-236.

Rosati, F., Selmi, G., and Mazzini, M. 1976. Comparative observations on the mitochondrial derivatives of insect sperm. J. Submicrosc. Cytol. 8: 51-67.

Smith, S. G., and Brower, J. H. 1974. Chromosome numbers of stored-product Coleoptera. J. Kansas. Entomol. Soc. 47: 317-319.

Suja, J. A., Vega C. G. De La, and Rufas, J. S. 1987. Meiotic stability of B chromosomes and production of macrospermatids in *Aiolopus strepens* (Orthoptera: Acrididae). Genome 29: 5-10.

Suja, J. A., Vega C. G. De La, and Rufas J. S. 1989. Mechanisms promoting the appearance of abnormal spermatids in B-carier individuals of *Euprepocenemis plorans* (Orthoptera). Genome 32: 64-71.

Werner, M., and Simmons. L. W. 2011. Ultrastructure of spermatozoa of *Onthophagus taurus* (Coleoptera, Scarabaeidae) exhibits heritable variation. Naturwissenschaften 98: 213-23.

Wolf, K. 1997. The formation of accessory tubules in spermatids of the red firebug, *Pyrrocoris apterus* (Hemiptera: Pyrralidae). European J. Entomol. 94: 263-270.

Wolf, K., and Joshi, H. 1995. Microtubule organization and the distribution of g-tubulin in spermatogenesis of a beetle, Tenebrio molitor (Tenebrionidae, Coleoptera, Insecta). J. Cell Sci. 108: 3855-3865.